ELSEVIER

International Journal of Mass Spectrometry 192 (1999) 327–345

International Journal of Mass Spectrometry

Femtosecond laser interactions with methyl iodide clusters. 2. Coulomb explosion at 397 nm

J.V. Ford, L. Poth, Q. Zhong, A.W. Castleman Jr.*

Department of Chemistry, The Pennsylvania State University, 152 Davey Laboratory, University Park, PA 16802, USA

Received 18 September 1998; accepted 7 June 1999

Abstract

As a continuing effort to elucidate the effects of the interaction of femtosecond laser radiation with clusters, we have extended our studies of Coulomb explosion to a determination of the role of laser wavelength on the process. In the present study, the interactions of methyl iodide clusters, formed in a supersonic expansion using argon and helium as carrier gases, were investigated at 397 nm using a Ti:sapphire femtosecond laser. These studies are a continuation of the work initiated on methyl iodide clusters using 795 nm ionization. The resulting atomic and cluster ions were analyzed in a reflectron time-of-flight (TOF) mass spectrometer. Based on a comparison of the current results and those presented for 795 nm ionization, several suggested mechanisms to account for the formation of highly charged species and their concomitant Coulomb explosion are examined. The resulting analysis indicates that the Coulomb explosion of methyl iodide clusters has characteristics of several of the proposed models to account for the phenomenon, but cannot be fully explained by any one of them. (Int J Mass Spectrom 192 (1999) 327–345) © 1999 Elsevier Science B.V.

Keywords: Femtosecond lasers; Clusters; Coulomb explosions; Ions

1. Introduction

With the development of ultrafast lasers having temporal pulse widths in the picosecond and femtosecond time regimes, a new area of research has developed to probe the interaction of these laser pulses with matter. The generation of multiply charged species through multiphoton ionization of rare gas atoms and simple molecules using picosecond laser systems was first observed about 15 years ago [1–4]. Lompré and co-workers found that charge states as high as He^{2+} and Ne^{5+} were formed [1,2]. Using larger atomic mass species, higher charge states such as Ar^{8+} and Xe^{9+} were observed under high laser fluence conditions [3,4]. The next step in this emerging field involved study of simple diatomics such as N_2, HI, CO, H_2, and O_2 using both femtosecond and picosecond lasers [5–12]. Extensive studies on the N_2 molecule generated charge states as high as +4, and the atomic ions formed exhibited small kinetic energy releases due to electrostatic repulsion effects [5–7]. Studies on the HI molecule [8] generated charge states as high as I^{5+}. In all the isolated molecule systems, the kinetic energies of the atomic ions generated did not exceed several tens of electron volts. In other studies, larger systems were also examined at lower laser intensities, namely poly-

* Corresponding author. E-mail: AWC@psu.edu

PII S1387-3806(99)00131-1

atomic molecules such as UF_6 and solid targets [13–15]. Studies on UF_6 by Armstrong and co-workers [13], revealed the formation of uranium charge states as high as +3. The ions generated from solid targets had a much wider energy distribution with energies as high as several thousand electron volts.

Recently, investigations of laser-matter interactions have focused on using atomic and molecular clusters as the target of the intense laser beams [16–25]. The creation of multiply charged atomic ions in clusters typically gives rise to Coulomb explosion, where highly charged species formed in close proximity within a cluster experience strong Coulomb repulsion forces. Once the Coulomb repulsion exceeds the total cohesive energy of the cluster, the highly ionized cluster explodes into atomic and molecular fragments with varying charge states and relatively large kinetic energies. Rhodes and co-workers, using relatively high laser fluences similar to those used for the isolated molecule experiments, found that clusters or rare gas atoms undergoing Coulomb explosion also release x rays as part of the process [21,22]. Unlike the work on isolated atoms and molecules, the laser fluences used by Castleman and co-workers, in the first studies on molecular clusters, were only on the order of 10^{14} or 10^{15} W/cm^2. Using these moderate fluences, the HI system [16] generated iodine charge states as high as +17. The average kinetic energies associated with these ions was on the order of several hundred electron volts, clearly indicating that clusters present a unique platform on which to study matter-laser interactions. Additional work on the ammonia cluster system [20] indicated that intact cluster ions may also undergo Coulomb explosion. In very recent work, Ditmire and co-workers [23–25] have observed charge states as high as +40, with ion kinetic energies on the order of 1 MeV for large noble gas clusters. Unfortunately, the mechanism behind the Coulomb explosion process is not yet fully understood.

In an effort to explain the Coulomb explosion of clusters, in particular the mechanism, several theories have been put forth. One, by Rhodes and co-workers, is called the coherent electron motion model (CEMM) [21,22,26,27]. A second, by Rose-Petruck and co-workers is called the ionization ignition model (IIM) [28,29]. The observed high charge states and large ion energies could not be adequately explained by the usual ionization processes such as the above threshold multiphoton ionization [30], barrier suppression ionization [31,32], or tunneling ionization [31–33]. The failure of both the barrier suppression and the tunneling ionization mechanisms relate to the intensity of the laser beam being used. Keldysh defined a unitless parameter (γ) to distinguish between a multiphoton ionization (MPI) and tunneling process [33–35]. The equation is:

$$\gamma = \frac{\omega(2m_e\mathrm{IP})^{1/2}}{eE_o} \quad (1)$$

where ω is the laser frequency, m_e is the charge on the electron, IP is the ionization potential, e is the charge on the electron, and E_o is the electric field strength of the laser. Tunneling occurs when $\gamma < 1$, and MPI occurs when $\gamma \gg 1$. In general, the studies on cluster systems all have $\gamma \ll 1$, indicating that a tunneling process is likely to be operative. It should be noted that barrier suppression ionization is not a true MPI process, and both barrier suppression and tunneling ionization could be occurring. The laser fluences used by Castleman and co-workers are below the fluence regime considered necessary to generate the high charge state distribution observed. Therefore, a different mechanism for the generation of the high charge state atomic ions from clusters is required. Several questions need to be addressed when comparing the IIM and CEMM, among other mechanisms: What is the nature of the fragmentation? Does the process change with wavelength? How does laser fluence effect the system? Does cluster size or mass of the cluster components alter the Coulomb explosion?

The IIM is based on classical trajectory Monte Carlo simulations. The initial ionization event creates several ion cores within the cluster. During ionization, the electrons are ejected, leaving the ion cores confined within the cluster. The ion cores and the electric field of the ultrafast laser pulse interact to generate an inhomogeneous electric field throughout the cluster.

The combined field of the laser beam and the ion cores then suppress the ionization barrier within the cluster, thereby allowing additional electrons to be ejected, leading to an increase in the charge state of the ion cores. New ion cores can also be created in this fashion, which then interact with the laser beam. This increases the effective field and lowers the ionization barrier further, a process that continues until the cohesive energy of the cluster is no longer greater than the Coulomb repulsion forces, and Coulomb explosion occurs.

The IIM implies that cluster Coulomb explosion is asymmetric because it is unlikely that all of the species in the cluster, either atoms or molecules, will be ion cores. In addition, it is expected that cluster size will not have a large effect on the Coulomb explosion process. Along the same lines, changing the mass of the monomers in the cluster should only have a minimal effect. The formulation indicates that as the laser fluence is increased more charge states will be observed, and the number of ions generated will increase. However, if the required fluence threshold is not surpassed, Coulomb explosion does not occur, even with very short wavelengths.

The observation of hard x rays emitted when rare gas clusters were irradiated with intense laser fields on the order of 10^{19} W/cm^2 led to the development of CEMM [21,22,36]. The formation of x rays indicates that inner shell electrons have been lost from atoms within the cluster. In the formulation of this model, the loss of these inner shell electrons is attributed to collisions of the ejected electron with other electrons in the system. Electron collisions of this type may result in higher charge states. Irradiation of clusters by an ultrafast laser pulse, which has very intense electromagnetic fields, leads to an ionization regime where the loss of several electrons occurs on the same time scale as ejection of a single electron. It is assumed that the electrons initially removed by the laser begin to move coherently around the charged cluster, in response to the fields of the laser, thereby creating a quasiparticle. This quasiparticle is composed of the positively charged cluster as the nucleus, and the electrons have behavior similar to that of atomic orbits. The net effect of these interactions is that further ionization can occur by electron stripping, similar to high-energy electron impact ionization, leading to increased charge states in the quasi-nucleus (the positively charged cluster). The result of such high charge states in the quasi-nucleus is Coulomb explosion.

The CEMM, therefore, implies that as the wavelength of the ultrashort pulse decreases, the cluster fragmentation due to Coulomb explosion and the number of charge states generated increases. However, changing the laser fluence while maintaining the same ionization wavelength should have only a minimal effect. Furthermore, increasing the mass, and therefore the electron density of the cluster should facilitate explosion. Another implication of the model is that the fragmentation pattern might be expected to have a discernible pattern because all ion products are generated from the quasinucleus.

Recently, Ditmire and co-workers have presented an alternative explanation for the observation of x-ray production in clusters [23]. Instead of removing electrons from the inner shells of molecules in the cluster by electron impacts caused by coherent motion, the laser-matter interaction is suggested to create a very hot plasma. As the high energy electrons leave the plasma, they interact with electrons on the remaining atoms, removing the inner shell electrons. Electrons in the outer valence shells then fill these vacancies that generate the x rays. To date this model has been applied only to very large rare gas systems. Furthermore, several research groups have put forth other theories that are similar to the general concepts within the IIM [37–44], and some have proceeded beyond the assumptions first made in its formulation. These groups have asserted that when charge resonant states in the cluster are strongly coupled to the intense electromagnetic fields of the ultrafast pulse, high charge states are observable. Specifically, the groups of Bandrauk [37–39] and Corkum [40–42] deal with the motion, or frequency of the electrons between charged bodies, when an inner potential is applied to the system. Because both research groups use a quantum mechanical formulation, the effects of the inner potential on the molecular system require that the system have a locked or frozen geometry. As the

internuclear distance between charged bodies increases, at the critical internuclear separation the frequency of the electron motion in the inner potential becomes close to the frequency of laser radiation being utilized. When this condition occurs, the energy of the electron is increased through interaction of the light with the electron (a charge-resonance enhancement) resulting in the electron energy becoming larger than the height of the electrostatic inner barrier. When the electron energy is higher than the inner potential, the electron is removed from the system. This process increases until the Coulomb repulsion forces cause the system to Coulomb explode into charged atomic elements. This mechanism has been termed charge resonance enhanced ionization (CREI).

Recently, Jortner and co-workers [43,44] have taken this method and treated the concepts of CREI in a classical manner, allowing the structure of the system to be changed during irradiation. This formulation results in an inner barrier that is always rising in time, and may trap an electron on one side of the potential or another. When the applied field is reversed, the electron is able to overcome the inner potential, i.e. the electron "jumps" over the potential, with a net gain in electron energy from interaction with the field. The resulting enhancement of the electron energy can be quite large when several such jumps occur. Generally, the jumping repeats until the energy of the electron is higher than the inner potential, resulting in an increased charge state. Jortner and co-workers [43,44] have examined this mechanism in terms of single molecules and HI-Ar van der Waals clusters.

One of the key differences in the two general classes of models outlined above is the effect of laser wavelength on the Coulomb explosion process. The results presented previously on 795 nm ionization [45] seem to indicate that the mechanism behind Coulomb explosion of methyl iodide clusters may be a combination of features representative of both the IIM and CEMM models. In an effort to gain further information about the general mechanism behind the Coulomb explosion process, and to provide a database for assessing other promising approaches to this problem, clusters of methyl iodide seeded in argon and helium carrier gases have been investigated. The cluster beam was interrogated using 397 nm radiation from a femtosecond laser. In this article the effects of changing the wavelength are probed in terms of the energetics of the atomic ions generated. The response of the Coulomb explosion products to changes in laser power and the differences in the Coulomb explosion when the carrier gas is changed from argon to helium are also examined.

2. Experimental

The reflectron time-of-flight (TOF) apparatus and laser system used in this study have been described in previous publications [45–48]. Briefly, neutral clusters are generated by expanding a mixture of ~10% methyl iodide in either argon or helium carrier gas at a pressure of ~3000 Torr through a pulsed nozzle affixed with a 150 μm orifice. The neutral clusters are ionized and Coulomb exploded using the second harmonic output (397 nm) of a commercially available Ti:sapphire regeneratively amplified laser system that is focused by a 50 cm plano-convex lens into the center of the TOF source region. Following ionization, the ions are accelerated with a dual stage electrostatic field oriented perpendicular to both the molecular beam and laser axes. Following acceleration, the ion beam typically has ~4300 eV of translational energy and is collimated by a set of Einsel lenses and then admitted into the first field free region of the spectrometer. After exiting the field free region, the ions enter a reflectron. The reflectron acts as an electrostatic mirror, reflecting the ions through a second field free region toward a chevron microchannel plate (MCP) detector at a deflection angle of 1.5° relative to the initial ion beam. Time-of-flight mass spectra are recorded on a digital oscilloscope, after averaging for at least 1000 laser shots, and transferred to a personal computer for analysis.

Methyl iodide, a liquid at room temperature, has a vapor pressure of approximately 275 Torr. The liquid sample is obtained from Aldrich (98% pure) and the vapor pressure of the liquid is used to form the expansion gas mixture. Because of the low vapor

pressure of methyl iodide, the upper limit of the mixing ratio is ~10%. The carrier gases are obtained from MG Gas and have a purity of 99.5%. Methyl iodide vapor and carrier gas are mixed in a stainless steel mixing vessel and expanded at a backing pressure of ~3000 Torr. All gases were used without additional purification.

In brief, the laser system is composed of a Tsunami Ti:sapphire oscillator pumped by a CW argon ion laser, generating a mode-locked pulse train at 82 MHz with a pulse duration of ~56 fs and a pulse energy of 7 nJ. The pulses are seeded into a regenerative amplifier using a Ti:sapphire crystal as a gain medium, that in turn is pumped by the second harmonic (532 nm) of a 10 Hz Nd:YAG laser resulting in an output pulse with a temporal width of ~128 fs and an energy of 3.5 mJ. Note, these measurements are performed using the fundamental wavelength set at 795 nm. Following amplification and recompression, the fundamental beam is passed through a thin (1.5 mm) antireflection coated doubling crystal (KDP) generating the second harmonic at 397 nm. The temporal pulse width of the beam is assumed to be that of the fundamental and has an energy of 1.25 mJ per pulse.

For these experiments, the spectrometer is operated in a hard reflection mode. In this case the energy focusing effects of the reflectron are minimized by setting the first charged plate (U_t) at a potential greater than the birth potential (U_o) of the ions produced by the ionization. Typically, the voltage on U_t was set between 4900 and 6000 V. Coulomb explosion in the TOF assembly generates ions in all directions. The only ions detectable in our spectrometer are those ejected toward the reflectron along the spectrometer axis and those moving directly away from the reflectron toward the repeller plate (U_1) and turned via the applied potential on U_1. The experimental acceptance angle of the detected beam is less than 1° deflection from the TOF axis. The observed mass spectral peaks, for species undergoing Coulomb explosion, is composed of a feature representing ions ejected towards the detector initially, and a second feature at longer arrival times that represents species ejected toward the repeller plate that are stopped by the electrostatic field and reaccelerated towards the detector. The earlier arrival time feature is broad whereas the latter arrival time portion has been energy focused in the repeller region and is quite sharp. Self-focusing of the backward ejected ions means that, for a given atomic ion, higher kinetic energy ions have the same arrival time as lower kinetic energy ions. The self-focusing of this peak is due to the configuration of the spectrometer and the voltages applied in the TOF source.

Fig. 1 shows the two experimentally observed peak shapes. The difference between the peak shapes can be related to the kinetic energies of the ions. In the "classic" shape the energy distribution is not as large, whereas in the "shifted" shape the kinetic energies are much higher. The higher kinetic energies of Coulomb explosion increase the spacing between the forward and backward ejected ions. The increase in the intensity of the forward peak relative to the backward peak is due, at least to some extent, to loss of ion signal for the ions ejected backward. These ions, due to large kinetic energies, cannot be stopped by the spectrometer and annihilate on the repeller plate (U_1).

Two methods were used to determine the kinetic energies of the ions produced in the Coulomb explosion. The first method is to measure the peak splitting, which may be directly related to the kinetic energy released during Coulomb explosion, utilizing the following equation [20]:

$$\mathrm{KE} = \frac{(U_1 - U_2)^2}{8md^2} q^2 \Delta t^2 \tag{2}$$

where U_1 and U_2 are the voltages on the repeller and acceleration plates of the TOF source, m is the mass of the ion in u, d is the distance between U_1 and U_2 in meters, q is the product of the fundamental electric charge multiplied by the number of missing electrons in the ion, and Δt is the peak splitting in microseconds. Eq. (2) gives the kinetic energy in joules, but by using the unit conversion factor, $1\ \mathrm{eV} = 1.6021892 \times 10^{-19}$ J, the energy can be converted to electron volts. Alternatively, the cutoff method [49] is also used to determine the ion energies. Briefly, this method is employed by plotting the integrated peak

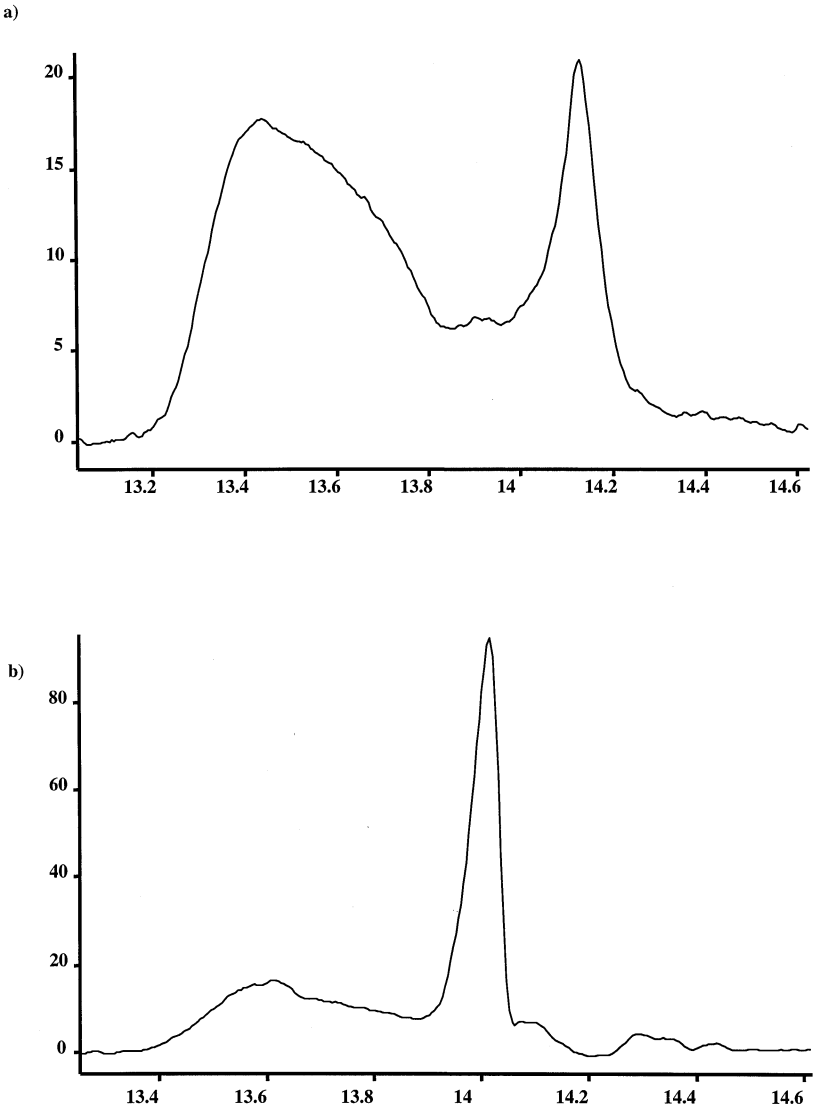

Fig. 1. (a) "Shifted" Coulomb explosion peak shape and (b) "classic" Coulomb explosion peak shape. Both these peaks were observed for methyl iodide in both argon and helium carrier gases. The *x* axis is ion arrival time (in μm s) and the *y* axis is spectral intensity (in mV).

intensity of a given mass peak versus the applied cutoff potential. The experiment decrements U_t from its starting value, in fixed voltage steps until the voltage on U_t is lower than the birth potential of the cluster ions observed in the mass spectrum. The midpoint of the resulting curve is taken as the kinetic energy of the ion. For the cluster ions observed, the midpoint represents the birth potential, whereas the atomic ion value represents the birth potential plus the kinetic energy gained by the ion during Coulomb explosion. Both of these methods are discussed further in the following sections.

The experimental effects of timing variation and focus position mapping of the neutral packet were performed at 397 nm and are in accord with the results obtained at 795 nm [45] and are therefore not reported

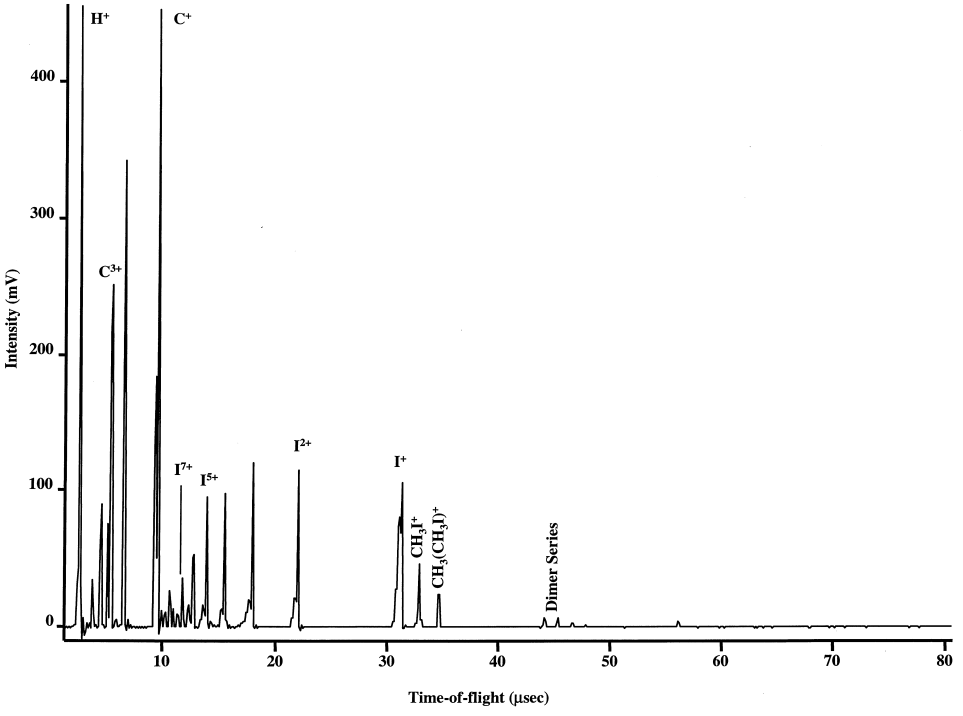

Fig. 2. Typical mass spectrum of Coulomb explosion of methyl iodide clusters at 397 nm in argon carrier gas. H^+ is truncated.

herein. It should be noted that, as in the case of 795 nm results, Coulomb explosion only occurs when clusters are present in the molecular beam.

3. Results: methyl iodide clusters in argon carrier gas

Fig. 2 shows a typical TOF mass spectrum for the Coulomb explosion of methyl iodide clusters in argon carrier gas using 397 nm ionization. Note that the cluster ion intensity is very small when compared to the atomic ions, implying that formation of atomic ions is preferred in the Coulomb explosion process. Additionally, the maximum charge state observed is +7 for iodine and +4 for carbon. Furthermore, the iodine mass peaks have a "classic" peak shape for charges +1 through +4, whereas charges +5 through +7 have a "shifted" peak shape. Additionally, the carbon ions all have a "shifted" peak shape. The maximum charge state observed for ionization with 795 nm radiation was +15 for iodine under similar expansion conditions, i.e. a mixing ratio of ~10% methyl iodide to argon, by pressure, at approximately 3000 Torr backing pressure. Under these conditions the iodine ions typically had a "shelf" peak shape [45]. Close examination of the mass spectrum shows that the hydrocarbon fragments CH_2^+ and CH_3^+ exhibit a Coulomb explosion peak shape. This observation occurs in approximately 50% of the mass spectra taken, and was never observed in the case of 795 nm ionization [45]. The largest cluster observed is $I(CH_3I)_3^+$, and the dominate cluster series is $I(CH_3I)_n^+$ for $n = 1$–3. In comparison, the dominate cluster series was also $I(CH_3I)_n^+$; however, the sizes ranged up to $n = 5$, which was also the largest cluster size observed.

The energetics of this system were examined using peak splitting and cutoff analysis as outlined above. In order to minimize the effects of day-to-day drift in our experimental setup, mainly due to differences in pulse

Table 1
Kinetic energies of the atomic ions generated from the Coulomb explosion of methyl iodide clusters in argon carrier gas. All energies and error values are in electron volts

Atomic ion	Peak splitting energy[a]	Cutoff energy[b]	Maximum kinetic energy (calculated)
C^{4+}	1168 ± 244	1116 ± 25	1483
C^{3+}	714 ± 110	657 ± 25	1046
C^{2+}	431 ± 106	378 ± 25	560
C^{+}	108 ± 38	109 ± 25	185
I^{7+}	1778 ± 321	763 ± 25	2123
I^{6+}	1251 ± 264	474 ± 25	1739
I^{5+}	883 ± 155	395 ± 395	1331
I^{4+}	520 ± 164	236 ± 25	835
I^{3+}	334 ± 133	147 ± 25	580
I^{2+}	112 ± 49	98 ± 25	306
I^{+}	12.0 ± 5.4	14.3 ± 11.6[c]	77

[a] The error values reported represent the standard deviation from eight peak splitting measurements.
[b] The errors reported represent the spread of the cluster birth potential measurements.
[c] In this case perhaps the standard deviation (11.6 eV) about the average birth potential was used.

nozzle and laser operation, only experiments conducted within a given day are directly compared. For this comparison, there are three to six experimental values for each atomic ion. Cutoff experiments are the most reliable because the integrated intensity versus cutoff potential is plotted and the kinetic energy value is read as the midpoint of the resulting curve. The birth potential was determined by averaging the cutoff potentials of the cluster ions detected, including the methyl iodide monomer ion. Two cutoff studies were conducted and averaged to give the reported experimental value. The error associated with this measurement represents the difference in the highest value and the average value reported. With few exceptions, the error outlined above is larger than any errors induced by the spread in the birth potential measurements determined from the cluster ions.

Additionally, by calculating where in time a non-Coulomb exploded highly charged ion should arrive, the experimental mass peak can be characterized by three regions: a broad feature representing the ions ejected toward the detector, a narrow peak centered at the calculated arrival time (referred to as the zero kinetic energy peak), and a narrow peak representing the self-focused ions ejected toward the repeller and then accelerated toward the detector. The center peak is given a pulse width based on the spectral peak width (at half maximum) of a non-Coulomb exploded cluster ion, using the following relation:

$$\frac{\Delta t_{\text{cluster}}}{t_{\text{cluster}}} = \frac{\Delta t_{\text{atomic ion}}}{t_{\text{atomic ion}}} \tag{3}$$

where Δt is the full width at half maximum and t is the arrival time of the species. Both Δt and t are measured in microseconds. Typically, the cluster ion chosen as the standard is $CH_3(CH_3I)^+$ which is the first molecular cluster peak not to exhibit a peak splitting commonly associated with Coulomb explosion. By subtracting the zero kinetic energy peak from the experimental spectral peak, the remaining two regions of the peak are elucidated. This peak fitting analysis allows the complete energy distribution of each atomic ion to be calculated, with the maximum kinetic energy value being the most significant. For a more detailed explanation of this method please see [45].

Table 1 summarizes all the kinetic energy values obtained. The maximum energies are taken from a number of different experiments and represent the largest observed kinetic energies. Examination of the mass peaks indicate that all the maximum values come from mass spectra where the kinetic energy distribution of a given species is shifted toward higher

values (i.e. the peaks have a "shifted" peak shape as discussed for Fig. 1). The most interesting aspect of Table 1 is the large discrepancy between the peak splitting and cutoff energies of the iodine ions beginning with +3. Detailed examination of the mass spectrum shown in Fig. 2 indicates a shift in peak shape at I^{5+}, but the energy results indicate that the shift in energy distribution really occurs at I^{3+}. Note that a magnification of the atomic ion region of the spectrum is required for this qualitative observation. Changes in the peak shape of an ion generated during a Coulomb explosion event should be indicative of changes in the energetics of the Coulomb explosion event. However, qualitative examination of the peak shape is not as sensitive to the energetics of the Coulomb explosion event as a peak splitting or cutoff measurement, which directly examines the energetics of the ion in question. Furthermore, the peak splitting and cutoff energies reported with 795 nm ionization [45] were generally smaller than those reported in Table 1, except for the cutoff energy when the maximum charge for iodine observed in the molecular beam was +15. These differences in energies are discussed further in Sec. 5.

The next series of experiments performed deals with the response of the ions generated by the Coulomb explosion process to changes in the laser power. Fig. 3(a) shows the integrated intensity response of the carbon ions. As expected each ion has an onset power, which in the case of C^{3+} and C^{4+} are very similar. The baselines of C^+ and C^{3+} are nonzero, which in the case of C^+ represents the background due to ionization of pump oil carbon. What is unclear is the reason for the nonzero baseline for C^{3+}. Fig. 3(b) gives the integrated intensity response of the iodine ions to changes in laser power. At first glance, this graph seems to indicate that each ion has a unique onset threshold. However, closer examination clearly indicates that I^{3+} and I^{4+} have the same onset threshold, as do I^{6+} and I^{7+}. [Fig. 3(c) shows an expanded intensity scale highlighting this observation.] The most surprising results from the power study are summarized in Fig. 4(a) and (b), which present the cluster ion intensity response. Instead of the cluster ion intensity peaking at low laser powers as reported in [45], the cluster signal smoothly declines until a baseline level is reached. The peak in the intensity reported in [45] occurred after the atomic ions generated during Coulomb explosion were no longer observable as the laser fluence was lowered, and it is unclear why the same result was not observed in the current studies below 7.5×10^{14} W/cm^2, which is the threshold value for the appearance of atomic ions generated from Coulomb explosion at 397 nm. These results are discussed further in Sec. 4.

4. Results: methyl iodide clusters in helium carrier gas

Fig. 5 shows a typical (TOF) mass spectrum for the Coulomb explosion of methyl iodide clusters in helium carrier gas. It is clear from the spectrum that the maximum charge state of iodine is +7 and that of carbon is +4. For ionization at 397 nm, the charge state distribution for both argon and helium carrier gases is the same, and is comparable to the helium system examined at 795 nm [45]. It is clear from examination of Fig. 5 that CH_3I^+ and I^+ are more intense than other atomic and cluster ions. This may be due to increased concentration of unclustered monomers in the molecular beam for the helium carrier gas case. As expected the dominate cluster ion series observed are $I(CH_3I)_n^+$ for $n = 0$–3. This cluster ion series is dominant in all carrier gases, at all ionization wavelengths, and for all mixing ratios. Unlike the 795 nm results where argon was observed to promote formation of larger cluster ions [45], the cluster ion distribution is similar for both carrier gases at this ionization wavelength. Furthermore, the cluster ions do not exhibit any type of peak splitting indicative of Coulomb explosion, which is in accord with the results for argon at this ionization wavelength and for the results presented in [45]. Close examination of the spectrum given in Fig. 5, displaying Coulomb explosion in helium carrier gas, shows that the hydrocarbon fragments CH^+ and CH_2^+ exhibit Coulomb explosion peak splitting; however, the CH_3^+ fragment does not. The peak splitting of these two hydrocarbon fragment ions indicates that they were formed during

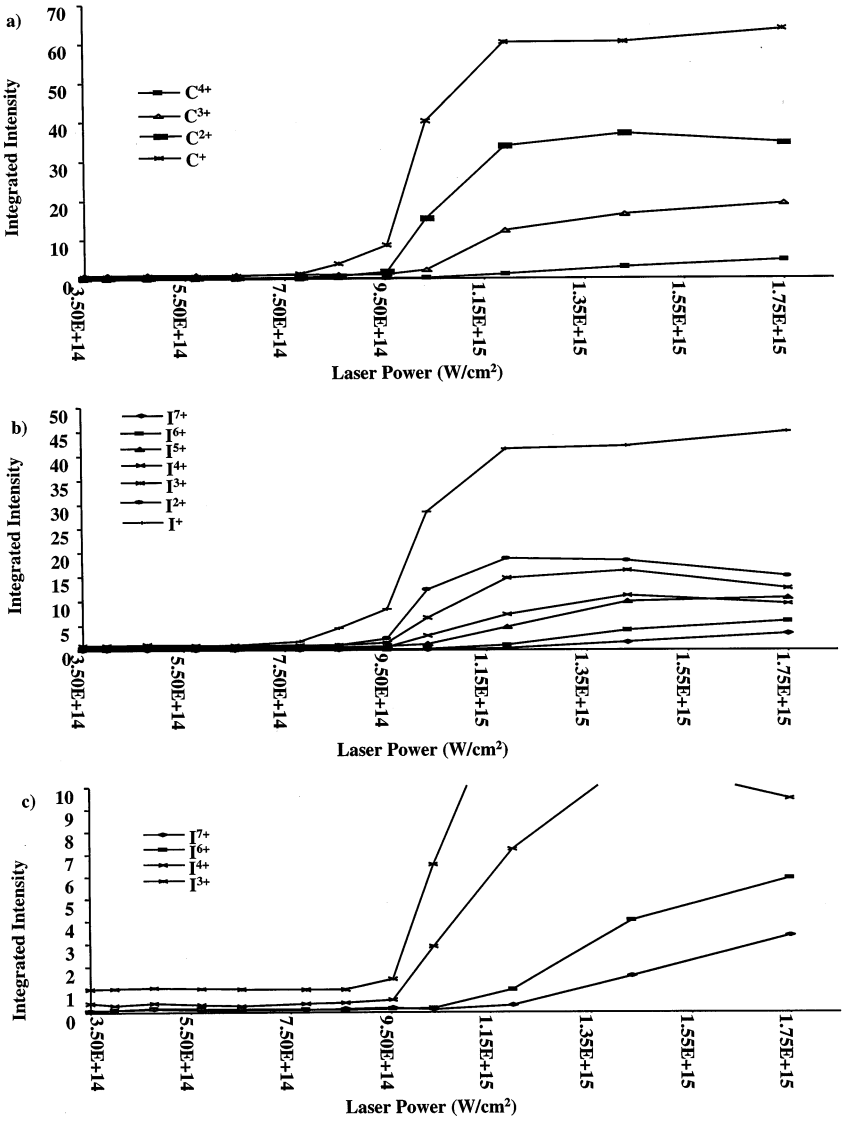

Fig. 3. Atomic ion responses to changes in laser ionization power. (a) Carbon ions, (b) iodine ions, and (c) iodine ions presented on an expanded intensity scale.

the Coulomb explosion of the clusters. Furthermore, because CH_3^+ is almost as intense as the C^+ ion, the methyl ion is almost certainly being formed during the Coulomb explosion process; what is unclear is why it does not exhibit peak splitting similar to CH^+ and CH_2^+. It should be noted at this time that residual CH_3^+ due to pump oil cannot account for these results and, furthermore, the large intensity attributable to CH_3^+ only occurs when Coulomb explosion is observed. Comparison of the peak heights of I^+ and CH_3^+ indicates that iodine is being converted into higher charge states. Additionally, the peak shapes of the iodine atomic ions favor the "classic" and "shifted" peak shapes, with I^{2+} through I^{5+} favoring the former and the higher charge states favoring the latter. The carbon ions all have a "shifted" peak shape. These

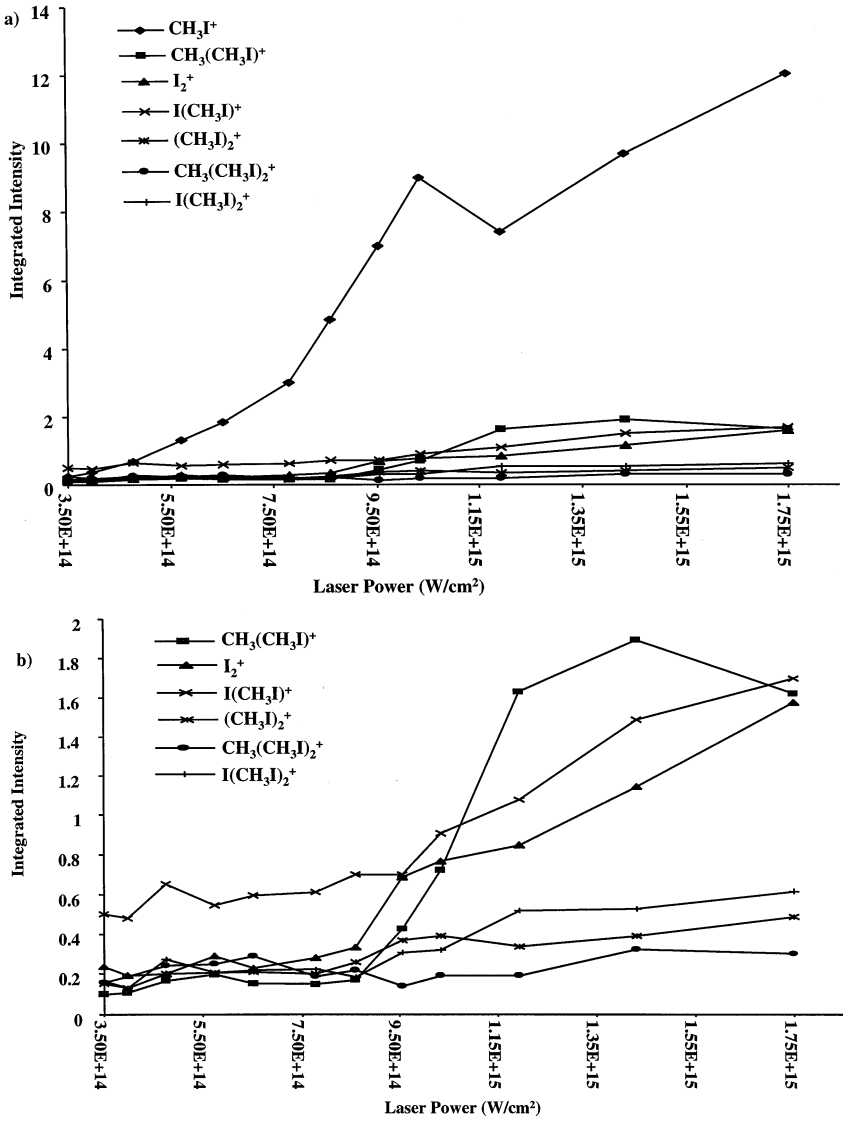

Fig. 4. Cluster ions intensity response to changes in laser power. Argon carrier gas. (a) All cluster ions shown, and (b) monomer cation removed to expand the intensity scale.

observations mimic the argon data presented above. These results differ from the observations at 795 nm in helium carrier gas where all peaks are characterized as having the "classic" peak shape [45].

The energetics of this system was examined using peak splitting analysis, cutoff analysis, and energy profiling as outlined above. The results of the energy analysis are summarized in Table 2. Unlike the argon results at this ionization wavelength and those presented in the preceding section, the cutoff energies and the peak splitting energies are about the same, within the error limits of the measurements, except for I^{7+}, C^{3+}, and C^{4+}. Furthermore, comparison of Tables 1 and 2 shows that, in general, the peak splitting energies measured from the argon carrier gas system are much larger than those found for the helium

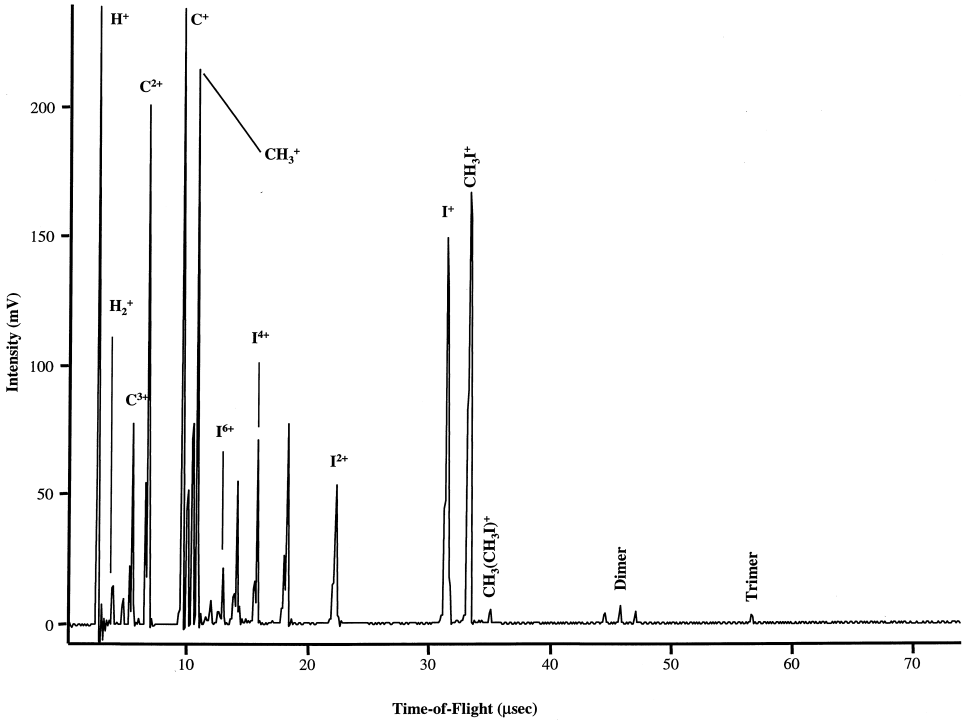

Fig. 5. Typical TOF mass spectrum for Coulomb explosion of methyl iodide clusters in helium carrier gas. H^+ is truncated to increase magnification.

system. This would tend to indicate that the two systems may have very different kinetic energy distributions. However, examination of the cutoff studies and the maximum kinetic energies indicate that the two systems should have similar energy distributions. The energies calculated from the peak splitting measurements are strongly dependent on the location of the maxima of the ion distribution attributable to the ions moving towards the detector. In the case of the argon carrier gas (at this ionization wavelength), the maxima is shifted to shorter arrival times, increasing the peak splitting kinetic energy release calculated. The shift in this maximum indicates that there are more ions generated with larger kinetic energies. However, this shift does not necessarily indicate an increase in the maximum kinetic energy observable.

In the cutoff experiment, the entire energy distribution is integrated and the average value of the distribution is determined. Since the cutoff kinetic energy values and the calculated maximum kinetic energy values are similar for both carrier gases, it may be inferred that the overall energy distribution is similar for both carrier gas systems at the 397 nm ionization wavelength. The difference in the peak splitting analysis may be attributed to the partitioning of ion energies, with the argon carrier gas case generating more ions with higher kinetic energies. This hypothesis is discussed further in the Sec. 5. Additionally, the results indicate that the peak splitting analysis, although useful as a qualitative tool, may not truly represent the energy distribution of the ion. As noted previously, the maximum energy values all represent mass spectra where the atomic ion is exhibiting a “shifted” peak shape, indicating that higher kinetic energy components are favored in the Coulomb explosion process.

The last series of experiments conducted with helium carrier gas were studies to investigate the effects of laser power. In general the atomic ion response is almost the same as outlined above for the

Table 2
Kinetic energies of the atomic ions generated from the Coulomb explosion of methyl iodide clusters in helium carrier gas. All energies and error values are in electron volts

Atomic ion	Peak splitting energy[a]	Cutoff energy[b]	Maximum kinetic energy (calculated)
C^{4+}	740 ± 160	1066 ± 156	1362
C^{3+}	491 ± 88	620 ± 74	951
C^{2+}	261 ± 54	338 ± 60	566
C^{+}	66 ± 29	99 ± 20	237
I^{7+}	1260 ± 149	886 ± 53	2136
I^{6+}	810 ± 145	699 ± 45	1768
I^{5+}	417 ± 99	483 ± 63	1385
I^{4+}	245 ± 51	336 ± 60	943
I^{3+}	111 ± 26	200 ± 38	603
I^{2+}	39.5 ± 13.8	108 ± 30	298
I^{+}	11.1 ± 5.7	34 ± 15	81

[a] The error values reported represent the standard deviation from four peak splitting measurements.
[b] Two cutoffs were averaged and the error reported is the standard deviation. The spread in cluster birth potentials for the two experiments was 30 and 35 V, which correspond to standard deviations of 12 and 15 V.

argon system. The carbon ion response exactly mimics the argon results with the threshold energies occurring at slightly higher laser power. In the case of the iodine ions shown in Fig. 6(a), the I^{5+} through I^{7+} ions have a common onset power level; also, the I^{3+} and I^{4+} ions have a single onset power as expected from the argon data. Whereas the cluster ion response in the argon system shows a decline in intensity with decreasing laser power, the response for the helium system is dramatically different, as shown in Fig. 6(b). Clearly, the clusters exhibit an initial decline as the laser power is lowered, but then peak at a low power condition, and thereafter disappear once the laser power is so low that ionization is no longer occurring. The rise at relatively low laser powers occurs when all the atomic ions with a charge greater than +1 are no longer being formed. This observation is consistent with the power studies presented for 795 nm ionization [43], which have the same general trend for the cluster ions observed.

5. Discussion and comparison

The first consideration that needs to be addressed for the Coulomb explosion of methyl iodide clusters is the ionization process. Table 3 clearly indicates that direct multiphoton ionization or processes such as barrier suppression cannot account for the large charge states observed. There are a couple of exceptions to this assertion—primarily the singly and charged ions when considering barrier suppression, as indicated by the following equation [50]:

$$I_{\text{th}} = 4.00 \times 10^9 \frac{E^4(\text{eV})}{Z^2} \quad (4)$$

where I_{th} is the laser intensity required for a given charge state, E is the ionization potential, Z is the charge state, and the leading constant corrects for units. At our maximum energy, the largest intensity obtained is $\sim 1.14 \times 10^{15}$ W/cm^2, which allows for the formation of only carbon ions with charge +1 and +2, whereas iodine may have charge states +1 through +3. The truncation of ionization at C^{4+} occurs because that is the point at which all the valence electrons in carbon have been removed. It should be noted, however, that although barrier suppression cannot explain the energy and charge state results alone, barrier suppression may help initiate the entire Coulomb explosion process.

The first series of comparisons is based on the mass spectra. In the case of 397 nm ionization, the

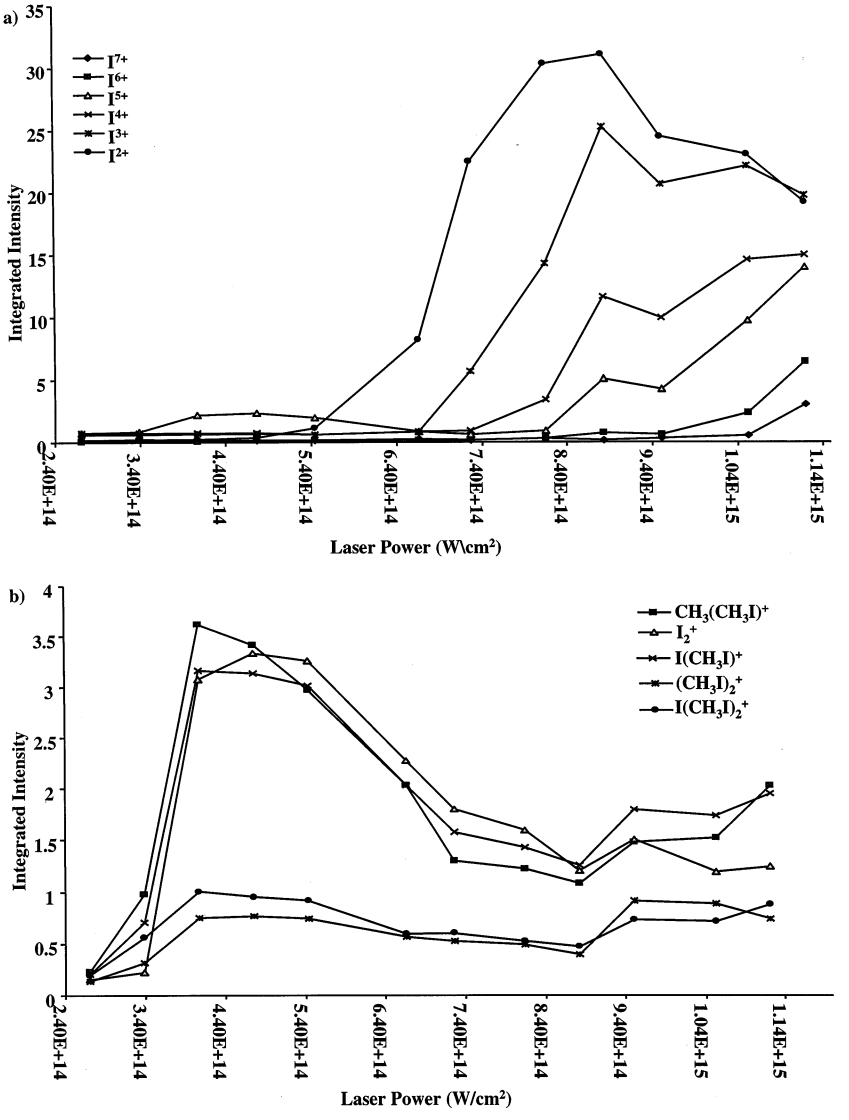

Fig. 6. Power studies of the methyl iodide clusters in helium carrier gas. (a) Iodine atomic ions and (b) cluster ions.

mass spectra of the two methyl iodide–carrier gas systems are very similar. The atomic ions all have a "classic" or "shifted" peak shape and the change from one peak shape to the other occurs at similar charge states ($\sim+4$) for the iodine atomic ions. Furthermore, the charge state distributions of the atomic ions were the same for both carrier gases. These observations are contrasted by the 795 nm results where the two methyl iodide–carrier gas systems had very different mass spectral characteristics, namely different charge state distributions and peak shapes [45]. This is a clear indication of a wavelength effect when moving from 795 nm to 397 nm ionization. This observation that a higher charge state distribution is observed for 795 nm ionization is not consistent with the CEMM, which predicts that bluer wavelengths should promote Coulomb explosion, as shown by the following equation [27]:

Table 3
Comparison of ionization potential and the number of photons required for simple multiphoton ionization leading to Coulomb explosion [51,52]. Note, these energies are stepwise in nature

Atomic ion	Ionization potential required to produce the given atomic ion[a]	Number of photons required to reach the ionization potential[b]
C^{4+}	64.492	21
C^{3+}	47.887	16
C^{2+}	24.383	8
C^{+}	11.260	4
I^{7+}	92.35	30
I^{6+}	78.84	26
I^{5+}	55.32	18
I^{4+}	44.01	15
I^{3+}	32.20	11
I^{2+}	21.40	7
I^{+}	10.59	4

[a] The IP values for carbon and argon were taken from [47], and the IP values for iodine were taken from [49].
[b] The energy per photon at 397 nm is approximately 3.11 eV.

$$N'_x = \tilde{\nu}_x n^{4/3}\left(\frac{2\tau c Z^2 \sigma_{ei}}{\lambda r_o^2}\right) \quad (5)$$

where N'_x is the number of ionization events, $\tilde{\nu}_x$ is a multiplicative factor modifying the average number of vacancies caused by each electron impact, n is the number of atoms in the cluster, τ is an approximation of the excitation time, c is the speed of light, Z is the charge, σ_{ei} is the inelastic cross section, λ is the ionization wavelength, and r_o is the interatomic spacing. Note that it is inferred that more ionization events should lead to higher charge states. However, this assertion is validated only for the argon system because the charge state distribution of the iodine ions is the same at both wavelengths for the helium system. What is also unclear is why the ion kinetic energies measured at 397 nm are generally larger than energies measured in [45] at 795 nm. It would appear that the carrier gas as well as the laser wavelength play an important role in the Coulomb explosion process.

One additional difference between the two carrier gas systems is also observed. In argon, the CH_3^+ fragment has a peak splitting, but in helium it is unsplit. However, in helium it is clearly being generated in the Coulomb explosion process because of its large intensity. If the methyl ion were in the background due to pump oil or formed from the photofragmentation of the methyl iodide monomer, the resulting ion signal would be less than the observed level. However, all three sources of the methyl ion contribute to the signal intensity observed in the mass spectrum. Once again, it would appear that argon is somehow affecting the Coulomb explosion process in such a way as to foster formation of higher energy methyl ions, producing the peak splitting. It should be noted that, in addition to the peak splitting, the intensity of the methyl ion in argon is much smaller. This decreased intensity may be attributable to preferential formation of carbon and hydrogen atomic ions during the Coulomb explosion event. From these results it is inferred that the argon carrier gas system is promoting an increase in methyl iodide clustering either through formation of a heterogeneous cluster or through an increase in the number of methyl iodide monomers coalescing into a neutral cluster.

Recently, Zeigler and co-workers [53] have calculated a stable dimer structure for methyl iodide in which the iodine atoms face one another with a nuclear separation of 3 Å. The methyl groups are found to angle away from the I · · · I axis at an angle of 115° resulting in a structure that is Z shaped. In the mass spectra for both ionization wavelengths the dominate cluster ion series is $I(CH_3I)_n^+$ for n = 1–3 or 5 depending on the carrier gas. The presence of

these species may indicate that the dimer is a building block of the cluster. Additionally, the presence of cluster ions I_2^+, $(CH_3I)_2^+$, and the presence of the methyl ion add support to this speculation.

Recall that in virtually all cases, the kinetic energies of the ions measured at 397 nm are larger than the values reported for 795 nm ionization [45]. Clearly, the shift toward larger kinetic energies represents some aspect of a wavelength dependent effect since the average energy per pulse (1.25 mJ versus ~3 mJ in [45]) is lower at 397 nm. The reason that the laser powers, in W/cm^2, are similar is that although the energy per pulse drops by a factor of ~3, the ionization spot size is reduced by a factor of ~4 when moving from 795 nm to 397 nm. The question now arises: which affects the energetics of the Coulomb explosion fragments more, fluence or wavelength? The CEMM asserts that bluer wavelengths promote Coulomb explosion, which is not consistent with the shift in charge state distributions discussed above, when moving from 795 nm to 397 nm ionization. The IIM asserts that as the fluence increases more Coulomb explosion occurs, consistent with the power studies presented. Neither model really makes an assertion as to how the energies of the resulting ions are affected by these changes in fluence or wavelength, although more Coulomb explosion could be interpreted as resulting in higher kinetic energies as well. Therefore, drawing conclusions as to which model best describes the Coulomb explosion process, with regard to changes in the energetics of the systems is problematic at best. Consequently, such conclusions will not be made. It might be more appropriate to discuss changes in the energetics of the process in terms of the carrier gases used.

Comparison of the energetics for the two carrier gas systems is intriguing. The argon system, for both ionization wavelengths, has energy values that are generally larger than the energies of the same Coulomb explosion products in helium carrier gas. This may be a good indication that argon serves to produce larger methyl iodide clusters, perhaps even creating a co-cluster of methyl iodide and carrier gas. In essence, some of the energy within the cluster is dissipated during the Coulomb explosion process by removal of the carrier gas species co-clustered with the methyl iodide cluster, increasing the energy required to Coulomb explode the cluster. In the case of the two carrier gases used, helium is very light and the intermolecular interactions between the methyl iodide cluster and the helium are weak with very little energy taken from the cluster by removal of the helium, if it is present at all in the initial neutral cluster. The results presented in Sec. 4 support this analysis because all the peak splitting and cutoff energies are similar. Argon, on the other hand, has a comparatively large mass with increased polarizeability that increases the strength of intermolecular attractions between the methyl iodide cluster and the argon. The removal of the argon from the co-cluster requires somewhat more energy. Because more energy is required, the ionization process within the cluster might continue to occur for a slightly longer period of time. This increase in laser-cluster interaction time could lead to the creation of higher charge states and/or additional ion cores increasing the Coulomb repulsion forces within the cluster leading to a more energetic explosion. The peak splitting results, which displayed larger kinetic energies for the argon carrier gas case, support this argument. This hypothesis assumes that the argon energy distribution is shifted to higher energies, and should lead to a higher maximum kinetic energy observed. Unfortunately, the cutoff and maximum kinetic energies of the argon and helium experiments are very similar, indicating a similar kinetic energy distribution. However, when taken together, the three energy measurements (peak splitting, cutoff, and maximum kinetic energy calculations) indicate that although the overall kinetic energy distributions are similar for both carrier gases, the argon case generates more ions in the higher energy side of the distribution. This interpretation supports the arguments above.

In light of the previous discussion, one of the more interesting results of the 397 nm experiments is the difference in the cluster ion responses to changes in laser power. Whereas the observations in [45] for both carrier gases are similar to the helium results presented herein, the argon results are intriguing. The 795 nm results [45] for both carrier gases, and the helium results reported herein, have the cluster ion

intensity peaking at low laser powers where the Coulomb explosion atomic ions are no longer being formed. However, for the argon system at 397 nm the cluster ion intensity simply falls to baseline without displaying peaking at the lower laser fluences, similar to the atomic ions. Furthermore, the power onsets for the atomic ions occur at lower energies in argon carrier gas. This observation may be the clearest indication that the argon carrier gas is present as a co-cluster of the carrier gas and the methyl iodide cluster. This enables the cluster to undergo a Coulomb explosion process that fragments the cluster into atomic ions, and a few cluster ions, even at laser powers barely above the ionization threshold. In the helium case, the carrier gas, if at all present in the cluster, is removed easily during the initial ionization. It should be noted that the carrier gas–methyl iodide interactions are individually much weaker than the energy of a single photon. At powers very near the methyl iodide monomer threshold, the lack of co-clustering leads to simple photofragmentation of the neutral methyl iodide cluster, resulting in the formation of cluster ions only, consistent with the analysis presented in Sec. 4.

One additional observation from the power studies needs to be discussed. In both carrier gases, several iodine charge states were found to share the same threshold energy. The fact that several charge states share one threshold level is not completely consistent with the IIM because the IIM only has a strong fluence dependence associated with the modified barrier suppression mechanism on which the model is based. However, this result at 397 nm is counter to the results at 795 nm [45] where a strong fluence dependence was observed that is consistent with the IIM. What is readily apparent from these results is that for redder wavelengths, fluence plays an important role in the formation of higher charge state species, whereas atomic ion fragments formed using a bluer wavelength have a much smaller charge state distribution and exhibit only a moderate fluence dependence. In this light, it is only safe to conclude that for methyl iodide Coulomb explosion, both models can partially explain the results. Perhaps by combining elements from both models, a better explanation of the Coulomb explosion mechanism may be postulated. However, as pointed out above, a possible new mechanism must also consider the effects of formation of co-clusters, composed of the carrier gas and the cluster species being examined.

6. Conclusions

This article has probed the effects of wavelength on the Coulomb explosion of methyl iodide clusters at 397 nm and compared them to the results obtained with 795 nm ionization [45]. The results indicate that there is both a wavelength and fluence effect present. In general, the observed effects due to wavelength are much stronger than the fluence effects. However, combined with the results in [45] for 795 nm ionization, it is apparent that redder wavelength experiments experience stronger fluence effects. Furthermore, this article has presented results that indicate that the carrier gas used in the cluster beam plays an important role in the Coulomb explosion process. In order to explain the results, neither the IIM nor the CEMM is sufficient. What is apparent is that once consideration of the carrier gas is included, elements of both models need to be combined to formulate a new model that better explains the Coulomb explosion process for methyl iodide clusters.

One aspect of the clustering process that was not directly discussed herein, but is discussed in [45], is that of cluster size. Although it is a powerful tool for probing the Coulomb explosion process, TOF mass spectrometry cannot address the size distribution of the neutral clusters being ionized by the laser beam. The co-clustering by carrier gas discussed in the Sec. 5 increases the overall cluster size of the system. In order to probe the effects of cluster size, a MS/MS approach or a series of molecular dynamics simulations would be of value. The latter approach is currently being considered, using the formulations of either Poth and Castleman [54] or of Jortner and co-workers [43].

Acknowledgement

The authors acknowledge the financial support of the Air Force Office of Scientific Research, Grant No. F49620-97-1-0183.

References

[1] L.A. Lompré, G. Mainfray, in Multiphoton Processes, L. Lambropoulos, S.J. Smith (Eds.), Springer-Verlag, Berlin, 1984, p. 23.
[2] A. l'Huiller, L.A. Lompré, G. Mainfray, C. Manus, Phys. Rev. A 27 (1983) 2503.
[3] U. Johann, T.S. Luk, I.A. McIntyre, A. McPherson, A.P. Schwarzenbach, K. Boyer, C.K. Rhodes, Proceedings of the Topical Meeting on Short Wavelength Coherent Generation, D.T. Atwood, J. Bokor (Eds.), AIP Conf. Proc. No. 147, AIP, New York, 1986, p. 157.
[4] T.S. Luk, U. Johann, H. Egger, H. Pummer, C.K. Rhodes, Phys. Rev. A 32 (1985) 217.
[5] K. Boyer, T.S. Luk, J.C. Solem, C.K. Rhodes, Phys. Rev. A 39 (1989) 1186.
[6] L.J. Frasinski, K. Codling, P. Hatherly, J. Barr, I.N. Ross, W.T. Toner, Phys. Rev. Lett. 58 (1987) 2424.
[7] C. Cornaggia, J. Lavancier, D. Normand, J. Morellec, H.X. Liu, Phys. Rev. A 42 (1990) 5464.
[8] K. Codling, L.J. Frasinski, P. Hatherly, J.R.M. Barr, J. Phys. B 20 (1987) L525.
[9] J. Lavancier, D. Normand, C. Cornaggia, J. Morellec, H.X. Liu, Phys. Rev. A 43 (1991) 1461.
[10] P.A. Hatherly, L.J. Frasinski, K. Codling, A.J. Langley, W. Skaikh, J. Phys. B: At. Mol. Opt. Phys. 23 (1990) L291.
[11] D. Normand, C. Cornaggia, J. Lavancier, J. Morellec, H.X. Liu, Phys. Rev. A 44 (1991) 475.
[12] K. Codling, L.J. Frasinski, P.A. Hatherly, J. Phys. B: At. Mol. Opt. Phys. 21 (1988) L433.
[13] D.P. Armstrong, D.A. Harkins, R.N. Compton, D. Ding, J. Chem. Phys. 100 (1994) 28.
[14] M.M. Murnane, H.C. Kapreyn, M.D. Rosen, R.W. Falcone, Science 251 (1991) 531.
[15] D.D. Meyerhofer, H. Chen, J.A. Delettrez, B. Soom, S. Uchida, B. Yaakobi, Phys. Fluids B5 (1993) 2584.
[16] J. Purnell, E.M. Snyder, S. Wei, A.W. Castleman Jr., Chem. Phys. Lett. 229 (1994) 333.
[17] A.W. Castleman Jr., E.M. Snyder, S.A. Buzza, J. Purnell, S. Wei, Proceedings of the Yamada Conference XLIII on Structures and Dynamics of Clusters, Frontiers Science Series No. 16, Universal Academy Press, Tokyo, Japan, 1996, p. 175.
[18] E.M. Snyder, S.A. Buzza, A.W. Castleman Jr., Phys. Rev. Lett. 77 (1996) 3347.
[19] S.A. Buzza, E.M. Snyder, D.A. Card, D.E. Folmer, A.W. Castleman Jr., J. Phys. Chem. 105 (1996) 7425.
[20] E.M. Snyder, S. Wei, J. Purnell, S.A. Buzza, A.W. Castleman Jr., Chem. Phys. Lett. 248 (1996) 1.
[21] A. McPherson, T.S. Luk, B.D. Thompson, K. Boyer, C.K. Rhodes, Appl. Phys. B57 (1993) 337.
[22] A. McPherson, B.D. Thompson, A.B. Borisov, K. Boyer, C.K. Rhodes, Nature 370 (1994) 631.
[23] T. Ditmire, T. Donnelly, R.W. Falcone, M.D. Perry, Phys. Rev. Lett. 75 (1995) 3122.
[24] T. Ditmire, J.W.G. Tisch, E. Springate, M.B. Mason, N. Hay, R.A. Smith, J. Marangos, M.H.R. Hutchinson, Nature 386 (1997) 54.
[25] Y.L. Shao, T. Ditmire, J.W.G. Tisch, E. Springate, J.P. Marangos, M.H.R. Hutchinson, Phys. Rev. Lett. 77 (1996) 3343.
[26] A.B. Borisov, J.W. Longworth, A. McPherson, K. Boyer, C.K. Rhodes, J. Phys. B: At. Mol. Opt. Phys. 29 (1996) 247.
[27] K. Boyer, B.D. Thompson, A. McPherson, C.K. Rhodes, J. Phys. B: At. Mol. Opt. Phys. 27 (1994) 4373.
[28] C. Rose-Petruck, K.J. Schafer, C.P.J. Barty, Appl. Laser Plasma Radiat. II, SPIE 2523 (1995) 272.
[29] C. Rose-Petruck, K.J. Schafer, C.P.J. Barty, Phys. Rev. A: At. Mol. Opt. Phys. 55 (1997) 118.
[30] R.R. Freeman, P.H. Bucksbaum, J. Phys. B: At. Mol. Opt. Phys. 24 (1991) 325.
[31] S. Augst, D. Strickland, D. Meyerhofer, S.L. Chin, J.H. Eberly, Phys. Rev. Lett. 63 (1989) 2212.
[32] F.A. Ilkov, J.E. Decker, S.L. Chin, J. Phys. B: At. Mol. Opt. Phys. 25 (1992) 4005.
[33] L.V. Keldysh, Sov. Phys. JETP 20 (1965) 307.
[34] L.A. Lompré, G. Mainfray, C. Manus, S. Repoux, J. Thebault, Phys. Rev. Lett. 36 (1976) 949.
[35] E. Mevel, P. Breger, R. Trainham, G. Petite, P. Agostini, A. Migus, J.P. Chambaret, A.A. Antonetti, Phys. Rev. Lett. 70 (1993) 406.
[36] A. McPherson, K. Boyer, C.K. Rhodes, J. Phys. B: At. Mol. Opt. Phys. 27 (1994) L637.
[37] T. Zuo, A.D. Bandrauk, Phys. Rev. A 52 (1995) 1.
[38] S. Chelkowski, A.D. Bandrauk, J. Phys. B: At. Mol. Opt. Phys. 28 (1995) L1.
[39] S. Chelkowski, T. Zuo, O. Atabek, A.D. Bandrauk, Phys. Rev. A 52 (1995) 2977.
[40] H. Stapelfeldt, E. Constant, P.B. Corkum, Phys. Rev. Lett. 74 (1995) 3780.
[41] T. Seideman, M.Y. Ivanov, P.B. Corkum, Phys. Rev. Lett. 75 (1995) 2819.
[42] E. Constant, H. Stapelfeldt, P.B. Corkum, Phys. Rev. Lett. 76 (1996) 4140.
[43] I. Last, I. Schek, J. Jortner, J. Chem. Phys. 107 (1997) 6685.
[44] I. Last, J. Jortner, Theoretical Study of Multielectron Dissociative Ionization Diatomics and Clusters in a Strong Laser Field, personal communication.
[45] J.V. Ford, Q. Zhong, L. Poth, A.W. Castleman Jr., J. Chem. Phys. (unpublished).
[46] L. Poth, Z. Shi, Q. Zhong, A.W. Castleman Jr., Int. J. Mass Spectrom. Ion Processes 154 (1996) 35.
[47] Z. Shi, S. Wei, J.V. Ford, A.W. Castleman Jr., Chem. Phys. Lett. 200 (1992) 142.
[48] J. Breen, K. Kilgore, W.B. Tzeng, S. Wei, A.W. Castleman Jr., J. Chem. Phys. 90 (1989) 11.

[49] S. Wei, A.W. Castleman Jr., Int. J. Mass Spectrom. Ion Processes 131 (1994) 223.
[50] S. Augst, D.D. Meyerhofer, D. Strickland, S.L. Chin, J. Opt. Soc. Am. B 8 (1991) 858.
[51] R.C. Weast (Ed.), CRC Handbook of Chemistry and Physics, CRC, Boca Raton, FL, 1989.
[52] T.A. Carlson, C.W. Nestor Jr., N. Wasserman, J.D. McDowell, At. Data 2 (1970) 63.
[53] P.G. Wang, Y.P. Zhang, C.J. Ruggles, L.D. Ziegler, J. Chem. Phys. 92 (1990) 2806.
[54] L. Poth, A.W. Castleman Jr., J. Phys. Chem. 102 (1998) 4075.